# $D^0$-$\bar{D}^0$ mixing sensitivity estimation at Belle II in wrong-sign decays $D^0 \to K^+\pi^-\pi^0$ via time-dependent amplitude analysis*

Long-Ke Li(李龙科)[1] Ye-Qi Chen(陈冶蕲)[2] Wen-Biao Yan(鄢文标)[3] Zi-Ping Zhang(张子平)[4]

University of Science and Technology of China, Hefei 230026, China

**Abstract:** The sensitivity of the $D^0$-$\bar{D}^0$ mixing parameters $x$ and $y$ is estimated in the wrong-sign decay $D^0 \to K^+\pi^-\pi^0$ by time-dependent amplitude analysis. The resolution of the $D^0$ lifetime is essential in time-dependent Dalitz analyses. The Belle II detector, which aims to collect a total integrated luminosity of 50 $ab^{-1}$ of data, has $\sigma = 140$ fs in Monte Carlo studies, a factor of two improvement over that of Belle and BaBar, so the produced Dalitz signal Monte Carlo samples are smeared with this resolution. Then a time-dependent Dalitz plot fitting is performed on these smeared samples, and the sensitivity of $D^0$-$\bar{D}^0$ mixing parameters are $\sigma_x = 0.057\%$ and $\sigma_y = 0.049\%$. These are about an order of magnitude improvement on current experimental results, without considering background effects.

**Keywords:** $D^0$-$\bar{D}^0$ mixing, sensitivity estimation, time-dependent amplitude analysis, wrong-sign decay, Belle II

**PACS:** 13.25.-k, 14.40.-n, 11.80.Fv **DOI:** 10.1088/1674-1137/41/2/023001

## 1 Introduction

All open-flavored neutral meson mixing phenomena, which mean oscillations between a particle and its anti-particle, $K^0$-$\bar{K}^0$, $B^0$-$\bar{B}^0$, $B_s^0$-$\bar{B}_s^0$, and $D^0$-$\bar{D}^0$, have been observed [1]. Among them, $D^0$-$\bar{D}^0$ mixing is the only up-type quark neutral meson system. Because the charm quark mass is special, neither small enough ($\ll \Lambda_{\rm QCD}$) nor large enough ($\gg \Lambda_{\rm QCD}$), $D^0$-$\bar{D}^0$ mixing is very hard to calculate via non-perturbative theory, and it can only rely on experimental measurements [2]. In the Standard Model (SM), $D^0$-$\bar{D}^0$ mixing has contributions from short distance interactions and long distance interactions. While the Cabibbo-Kobayashi-Maskawa (CKM) matrix and Glashow-Iliopoulos-Maiani (GIM) mechanism [3] strongly suppress $D^0$-$\bar{D}^0$ mixing to $< 10^{-3}$, long-distance and $SU(3)$ flavor breaking increase it to $10^{-2}$ [4]. If the magnitude of $D^0$-$\bar{D}^0$ mixing beyond the SM is observed, New Physics (NP) is implied. Measurements and studies of $D^0$-$\bar{D}^0$ mixing play a very important and fundamental role in precise tests of the SM and searching for NP.

Table 1 summarises the experimental status of $D^0$-$\bar{D}^0$ mixing and $CP$ violation. $D^0$-$\bar{D}^0$ mixing was first observed with more than five standard deviation ($5\sigma$) confidence level in the wrong-sign (WS) decay $D^0 \to K^+\pi^-$ [5–7]. LHCb gave the first observation of $D^0$-$\bar{D}^0$ mixing in the WS decay $D^0 \to K^+\pi^-\pi^+\pi^-$ [8]. The BaBar collaboration presented the first evidence of $D^0 \to K^+\pi^-\pi^0$ with $3.2\sigma$ via time-dependent amplitude analysis [9], but this result is still under the statistical limit.

Belle II will start its first physics runs in 2018 and aims to collect 50 $ab^{-1}$ of experimental data. It will be a wonderful platform to measure $D^0$-$\bar{D}^0$ mixing and $CP$ violation with more precision. The sensitivity estimation of $D^0$-$\bar{D}^0$ mixing and $CP$ violation in $D^0 \to K^0_S\pi^+\pi^-$ has already been presented by the Belle II collaboration [10]. In this paper, $D^0$-$\bar{D}^0$ mixing sensitivity in WS decay $D^0 \to K^+\pi^-\pi^0$ at the Belle II experiment is estimated.

## 2 Formalism of $D^0$-$\bar{D}^0$ mixing

Mixing results from the flavour eigenstates $|D^0\rangle(c\bar{u})$ and $|\bar{D}^0\rangle(\bar{c}u)$, which have a definite quark component, and the mass eigenstates $|D_1\rangle$ and $|D_2\rangle$ which have definite mass and lifetime. The time evolution of the $D^0$-$\bar{D}^0$ system can be described by the Schrödinger equation with effective Hamiltonian $\mathcal{H} = (\boldsymbol{M} - i\boldsymbol{\Gamma}/2)$ where $\boldsymbol{M}$ and $\boldsymbol{\Gamma}$ are mass and width Hermitian matrices, and $CPT$

Received 21 September 2016, Revised 14 October 2016

∗ Supported by National Natural Science Foundation of China (11475164, 11475169, 11675166)

1) E-mail: lilongke@mail.ustc.edu.cn

2) E-mail: chenyq15@mail.ustc.edu.cn

3) E-mail: wenbiao@ustc.edu.cn

4) E-mail: zpz@ustc.edu.cn

©2017 Chinese Physical Society and the Institute of High Energy Physics of the Chinese Academy of Sciences and the Institute of Modern Physics of the Chinese Academy of Sciences and IOP Publishing Ltd

Table 1. The experimental status of $D^0$-$\bar{D}^0$ mixing and $CP$ violation in different decays.

| decay type | final state | LHCb | Belle | BaBar | CDF | CLEO | BES III |
|---|---|---|---|---|---|---|---|
| DCS 2-body(WS) | $K^+\pi^-$ | ★ | ★ | ☆ | ★ | $\surd$ | $\surd_{\delta^{K\pi}}$ |
| $CP$-eigenstates | $K^+K^-$, $\pi^+\pi^-$ | $\stackrel{(a)}{\surd}_{A_{CP}}$ | ☆ | ☆ | $\surd_{A_{CP}}$ | $\surd$ | |
| DCS 3-body(WS) | $K^+\pi^-\pi^0$ | | $\surd_{A_{CP}}$ | ☆ | | $\surd_{A_{CP}}$ | |
| self-conjugated 3-body decay | $K^0_S\pi^+\pi^-$ | $\surd$ | $\surd$ | $\surd$ | $\surd_{A_{CP}}$ | $\surd$ | |
| | $K^0_SK^+K^-$ | | $\stackrel{(b)}{\surd}$ | $\surd$ | | | |
| self-conjugated SCS 3-body decay | $\pi^+\pi^-\pi^0$ | $\surd_{A_{CP}}$ | $\surd_{A_{CP}}$ | $\surd^{\text{mixing}}_{A_{CP}}$ | | | |
| | $K^+K^-\pi^0$ | | | $\surd_{A_{CP}}$ | | | |
| SCS 3-body | $K^0_SK^\pm\pi^\mp$ | | | | | $\surd_{\delta^{K^0_SK\pi}}$ | |
| semileptonic decay | $K^+l^-\nu_l$ | | $\surd$ | $\surd$ | | $\surd$ | |
| multi-body(n⩾4) | $K^+\pi^-\pi^+\pi^-$ | ★ | $\surd_{A_{CP}}$ | $\surd$ | | | |
| | $\pi^+\pi^-\pi^+\pi^-$ | $\surd_{A_{CP}}$ | | | | | |
| | $K^+K^-\pi^+\pi^-$ | $\stackrel{(c)}{\surd}_{A_{CP}}$ | | $\surd_{A_T}$ | | $\surd_{A_{CP}}$ | |
| $\psi(3770)\to D^0\bar{D}^0$ via correlations | | | | | | $\surd_{\delta^{K\pi}}$ | $\surd_{y_{CP}}$ |

★ for observation ($>5\sigma$); ☆ for evidence ($>3\sigma$); $\surd$ for measurement published. Here DCS(SCS) stands for the Doubly(Singly) Cabibbo Suppressed.

(a) LHCb also give a measurement of indirect $CP$ asymmetry in Phys. Rev. Lett. **112**, 041801 (2014).

(b) Belle measured $y_{CP}$ in $D^0\to K^0_S\phi$ in Phys. Rev. D **80**, 052006 (2009). A time-dependent amplitude analysis of this decay channel for mixing parameters $(x,y)$ is ongoing.

(c) LHCb have also searched for $CP$ violation using $T$-odd correlations in JHEP **10** (2014) 005.

invariance requires $M_{11}=M_{22}\equiv M$ and $\Gamma_{11}=\Gamma_{22}\equiv\Gamma$. The mass eigenstates propagate through space and time as the form of the mixture of two flavour eigenstates. The proper time evolution of the mass eigenstates is

$$|D_{1,2}(t)\rangle = p|D^0(t)\rangle \pm q|\bar{D}^0(t)\rangle = e_{1,2}(t)|D_{1,2}(0)\rangle \quad (1)$$

$$e_{1,2}(t) = e^{-i(m_{1,2}-i\Gamma_{1,2}/2)t} = e^{-iMt}e^{-\Gamma t/2}e^{\mp(ix+y)\Gamma t/2}, \quad (2)$$

where the term $e^{-iMt}$ factor is a pure phase which is common to both mass eigenstates, and can be canceled. The mixing parameters $x$ and $y$ in last term are defined with average width $\Gamma=(\Gamma_1+\Gamma_2)/2$.

$$x=\frac{m_1-m_2}{\Gamma}=\frac{\Delta M}{\Gamma}, \quad y=\frac{\Gamma_1-\Gamma_2}{2\Gamma}=\frac{\Delta\Gamma}{2\Gamma}. \quad (3)$$

The time-dependent amplitude of the decay of an initial pure flavor eigenstate $|D^0(t=0)\rangle$ to final state $|\bar{f}\rangle$ can be expressed as

$$\begin{aligned}\mathcal{M}(\bar{f},t) &= \langle\bar{f}|\mathcal{H}|D^0(t=0)\rangle \\ &= \frac{1}{2}\left[\left(\mathcal{A}_{\bar{f}}+\frac{q}{p}\bar{\mathcal{A}}_{\bar{f}}\right)e_1(t)+\left(\mathcal{A}_{\bar{f}}-\frac{q}{p}\bar{\mathcal{A}}_{\bar{f}}\right)e_2(t)\right], \quad (4)\end{aligned}$$

where $\mathcal{A}_{\bar{f}}=\langle\bar{f}|\mathcal{H}|D^0\rangle$ and $\bar{\mathcal{A}}_{\bar{f}}=\langle\bar{f}|\mathcal{H}|\bar{D}^0\rangle$, and the decay rate of $D^0\to\bar{f}$ is

$$\begin{aligned}|\mathcal{M}(\bar{f},t)|^2 = \frac{e^{-\Gamma t}}{2}\Bigg[&\left(|\mathcal{A}_{\bar{f}}|^2+|\frac{q}{p}|^2|\bar{\mathcal{A}}_{\bar{f}}|^2\right)\cosh(y\Gamma t) \\ &+\left(|\mathcal{A}_{\bar{f}}|^2-|\frac{q}{p}|^2|\bar{\mathcal{A}}_{\bar{f}}|^2\right)\cos(x\Gamma t) \\ &-2\cdot\mathrm{Re}\left(\frac{q}{p}\bar{\mathcal{A}}_{\bar{f}}\mathcal{A}^*_{\bar{f}}\right)\cdot\sinh(y\Gamma t) \\ &+2\cdot\mathrm{Im}\left(\frac{q}{p}\bar{\mathcal{A}}_{\bar{f}}\mathcal{A}^*_{\bar{f}}\right)\cdot\sin(x\Gamma t)\Bigg]. \quad (5)\end{aligned}$$

Equation(5) shows that $y$ changes the time information of the Dalitz plot, and $x$ introduces an oscillation in this amplitude.

Under the assumptions of $|x|,|y|\ll 1$ and $CP$ conservation $(q/p=1)$, $|\mathcal{M}(\bar{f},t)|^2$ is

$$\begin{aligned}|\mathcal{M}(\bar{f},t)|^2 = e^{-\Gamma t}\Bigg(&|\mathcal{A}_{\bar{f}}|^2+\frac{x^2+y^2}{4}|\bar{\mathcal{A}}_{\bar{f}}|^2(\Gamma t)^2-\mathrm{Re}(\mathcal{A}_{\bar{f}}\bar{\mathcal{A}}^*_{\bar{f}}) \\ &\cdot y\Gamma t-\mathrm{Im}(\mathcal{A}_{\bar{f}}\bar{\mathcal{A}}^*_{\bar{f}})\cdot x\Gamma t\Bigg). \quad (6)\end{aligned}$$

Figure 1 shows two processes for $D^0$ WS decay and right-sign (RS) decay. WS decay can be directly through a doubly Cabibbo suppressed (DCS) process, or a Cabbibo favored (CF) process produced by mixing. Both processes are analogous. For RS decay, a DCS process produced by mixing, relative to a CF process, is negligible.

For the WS decay $D^0\to K^+\pi^-\pi^0$, the Belle collaboration measured the ratio of rates for WS-to-RS decays as $R_{WS}=(0.229\pm0.015)\%$ [11]. The BaBar collaboration has determined the relative strong phase variation across the Dalitz plot, and reported effective mixing parameters [9] $x''=(2.61^{+0.57}_{-0.68}\pm0.39)\%$ and $y''=(-0.06^{+0.55}_{-0.64}\pm0.34)\%$ with $3.2\sigma$ significance, where $x''$ and $y''$ are defined as

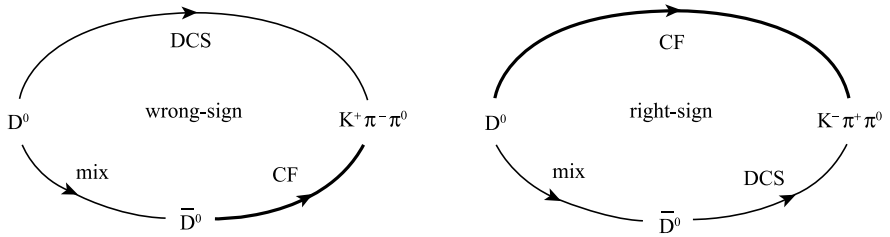


Fig. 1. WS decay (left) through the DCS process and mixing followed by the CF process, and RS decay (right) through the CF process and mixing followed by the DCS process.

$$x'' = x\cdot\cos\delta_{\mathrm{K}\pi\pi^0} + y\cdot\sin\delta_{\mathrm{K}\pi\pi^0},$$
$$y'' = y\cdot\cos\delta_{\mathrm{K}\pi\pi^0} - x\cdot\sin\delta_{\mathrm{K}\pi\pi^0}, \quad (7)$$

where $\delta_{\mathrm{K}\pi\pi^0}$ is the strong phase difference between the DCS $\mathrm{D}^0\to\mathrm{K}^+\rho^-$ and the CF $\bar{\mathrm{D}}^0\to\mathrm{K}^+\rho^-$ amplitudes and does not vary across the Dalitz plot. Here WS decay amplitudes for $\mathrm{D}^0$ or $\bar{\mathrm{D}}^0$ to final states $\bar{f}$ in Fig. 1 are defined [9] as:

$$\mathcal{A}_{\bar{f}}(m^2_{\mathrm{K}^+\pi^-},m^2_{\pi^-\pi^0}) = r_0\cdot\mathcal{A}^{\mathrm{DCS}}_{\bar{f}}(m^2_{\mathrm{K}^+\pi^-},m^2_{\pi^-\pi^0}), \quad (8)$$
$$\bar{\mathcal{A}}_{\bar{f}}(m^2_{\mathrm{K}^+\pi^-},m^2_{\pi^-\pi^0}) = \bar{\mathcal{A}}^{\mathrm{CF}}_{\bar{f}}(m^2_{\mathrm{K}^+\pi^-},m^2_{\pi^-\pi^0}). \quad (9)$$

Using Euler's relations to expand the strong phase $\delta_{\mathrm{K}\pi\pi^0}$, $|\mathcal{M}(\bar{f},t)|^2$ is rewritten as Eq.(10) under $CP$ conservation $(q/p=1)$,

$$\begin{aligned}|\mathcal{M}(\bar{f},t)|^2 = \mathrm{e}^{-\Gamma t}\Big\{ & r_0^2\cdot|\mathcal{A}^{\mathrm{DCS}}_{\bar{f}}|^2 + \frac{x''^2+y''^2}{4}|\bar{\mathcal{A}}^{\mathrm{CF}}_{\bar{f}}|^2(\Gamma t)^2 \\ & - r_0\cdot[y''\,\mathrm{Re}(\mathcal{A}^{\mathrm{DCS}}_{\bar{f}}\bar{\mathcal{A}}^{*\,\mathrm{CF}}_{\bar{f}}) \\ & + x''\,\mathrm{Im}(\mathcal{A}^{\mathrm{DCS}}_{\bar{f}}\bar{\mathcal{A}}^{*\,\mathrm{CF}}_{\bar{f}})]\cdot\Gamma t\Big\} \end{aligned} \quad (10)$$

where $r_0$ is the modulus of the relative complex number between the CF and DCS amplitudes, and $\mathcal{A}^{\mathrm{DCS}}_{\bar{f}}$ and $\bar{\mathcal{A}}^{\mathrm{CF}}_{\bar{f}}$ are normalized shapes on the Dalitz plot region. The effective mixing parameters $x''$ and $y''$ could be extracted by performing a time-dependent Dalitz plot fitting of the WS sample. The term $r_0^2$ in Eq. (10) can be absorbed into the normalizaiton of signal probability density function:

$$\begin{aligned} PDF_{\mathrm{sig}} = \frac{\mathrm{e}^{-\Gamma t}}{N}\Big\{ & |\mathcal{A}^{\mathrm{DCS}}_{\bar{f}}|^2 + \frac{c_1^2+c_2^2}{4}|\bar{\mathcal{A}}^{\mathrm{CF}}_{\bar{f}}|^2(\Gamma t)^2 \\ & - [c_1\cdot\mathrm{Re}(\mathcal{A}^{\mathrm{DCS}}_{\bar{f}}\bar{\mathcal{A}}^{*\,\mathrm{CF}}_{\bar{f}}) \\ & + c_2\cdot\mathrm{Im}(\mathcal{A}^{\mathrm{DCS}}_{\bar{f}}\bar{\mathcal{A}}^{*\mathrm{CF}}_{\bar{f}})]\Gamma t\Big\} \end{aligned} \quad (11)$$

where the normalized mixing parameters are $c_1 = y''/r_0$, and $c_2 = x''/r_0$ and $N$ is the normalization factor with

$$\oint_{\mathrm{DP}} \mathrm{d}m^2_{\mathrm{K}^+\pi^-}\mathrm{d}m^2_{\pi^-\pi^0} \cdot\int_{t_{\min}}^{t_{\max}}\mathrm{d}t PDF_{\mathrm{sig}}(m^2_{\mathrm{K}^+\pi^-},m^2_{\pi^-\pi^0},t) = 1. \quad (12)$$

## 3 Dalitz analysis

### 3.1 Isobar model

The three body decay of $\mathrm{D}^0\to\mathrm{ABC}$ happens through an AB resonance as shown in Fig. 2. The conservation of energy and momentum has

$$M^2_{\mathrm{D}^0}+M^2_{\mathrm{A}}+M^2_{\mathrm{B}}+M^2_{\mathrm{C}} = m^2_{\mathrm{AB}}+m^2_{\mathrm{BC}}+m^2_{\mathrm{AC}} = \text{constant}. \quad (13)$$

When a pseudoscalar meson decays to three pseudoscalar mesons, there are two degrees of freedom. Two of these three invariant mass-squares of final particle pairs can be the Dalitz variables in the standard form of the Dalitz plot:

$$\mathrm{d}\Gamma = \frac{1}{(2\pi)^3}\frac{1}{32M^3}\overline{|\mathcal{M}|^2}\mathrm{d}m^2_{\mathrm{AB}}\mathrm{d}m^2_{\mathrm{BC}}. \quad (14)$$

The width of each resonance is mass-dependent, given by:

$$\Gamma_{\mathrm{AB}} = \Gamma^{\mathrm{r}}_0\left(\frac{q_{\mathrm{AB}}}{q_{\mathrm{r}}}\right)^{2J+1}\left(\frac{M_{\mathrm{r}}}{m_{\mathrm{AB}}}\right)F^2_{\mathrm{r}} \quad (15)$$

where $m_{\mathrm{AB}}$ is the AB invariant mass (candidate), $M_{\mathrm{r}}$ is the nominal resonance mass, $J$ is the spin of the resonance, $\Gamma^r_0$ is the nominal width of the resonance, $q_{\mathrm{AB}}$ is the momentum of either daughter in the AB rest frame and $q_{\mathrm{r}}$ is the momentum of either daughter in the resonance rest frame, respectively, as follows:

$$q_{\mathrm{AB}} = \frac{1}{2m_{\mathrm{AB}}} \cdot\sqrt{[m^2_{\mathrm{AB}}-(M_{\mathrm{A}}+M_{\mathrm{B}})^2][m^2_{\mathrm{AB}}-(M_{\mathrm{A}}-M_{\mathrm{B}})^2]}, \quad (16)$$
$$q_{\mathrm{r}} = \frac{1}{2M_{\mathrm{r}}}\sqrt{[M^2_{\mathrm{r}}-(M_{\mathrm{A}}+M_{\mathrm{B}})^2][M^2_{\mathrm{r}}-(M_{\mathrm{A}}-M_{\mathrm{B}})^2]}. \quad (17)$$

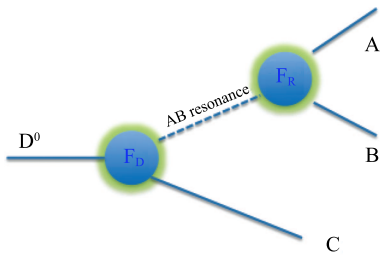


Fig. 2. Isobar model for resonances.

The amplitude for a spin-$J(J=0,1,2)$ resonance [12] is:

$$\mathcal{A}_J(\mathrm{ABC|r}) = F_\mathrm{D} \times F_\mathrm{r} \times T_\mathrm{r} \times \Omega_J. \tag{18}$$

Here the $T_\mathrm{r} \times \Omega_J$ is the resonance propagator. $T_\mathrm{r}$ is the dynamical function for the resonance $r$, and $\Omega_J$ is the angular momentum description dependent on the spin-$J$ of resonance $r$. The dynamical function $T_\mathrm{r}$ is commonly described using a relativistic Breit-Wigner (RBW) parameterization with mass-dependent width in Eq.(15).

$$T_\mathrm{r} = \frac{1}{M_\mathrm{r}^2 - m_\mathrm{AB}^2 - \mathrm{i}M_\mathrm{r}\Gamma_\mathrm{AB}}. \tag{19}$$

The angular dependence $\Omega_\mathrm{r}$ is described using either Zemach tensor formalism [13] as follows. The angular expressions $\Omega_J$ ($J=0,1,2$ respectively stands for scalar, vector and tensor intermediate resonance) are

$$\Omega_0(\mathrm{ABC|r}) = 1. \tag{20}$$

$$\Omega_1(\mathrm{ABC|r}) = m_\mathrm{AC}^2 - m_\mathrm{BC}^2 + \frac{(M_\mathrm{D}^2 - M_\mathrm{C}^2)(M_\mathrm{B}^2 - M_\mathrm{A}^2)}{M_\mathrm{r}^2}. \tag{21}$$

$$\begin{aligned}\Omega_2(\mathrm{ABC|r}) = &\left(m_\mathrm{BC}^2 - m_\mathrm{AC}^2 + \frac{(M_\mathrm{D}^2 - M_\mathrm{C}^2)(M_\mathrm{A}^2 - M_\mathrm{B}^2)}{M_\mathrm{r}^2}\right)^2 \\ &- \frac{1}{3}\left(m_\mathrm{AB}^2 - 2M_\mathrm{D}^2 - 2M_\mathrm{C}^2 + \frac{(M_\mathrm{D}^2 - M_\mathrm{C}^2)^2}{M_\mathrm{r}^2}\right) \\ &\times \left(m_\mathrm{AB}^2 - 2M_\mathrm{A}^2 - 2M_\mathrm{B}^2 + \frac{(M_\mathrm{A}^2 - M_\mathrm{B}^2)^2}{M_\mathrm{r}^2}\right).\end{aligned} \tag{22}$$

The form factor at the $\mathrm{D}^0$ produced vertex or decay vertex ($F_\mathrm{D}$ or $F_\mathrm{r}$) which attempts to model the underlying quark structure of the $\mathrm{D}^0$ meson or the intermediate resonances r, is parameterised by the Blatt-Weisskopf penetration factors for the particle with different spin $J$ as follows:

$$F_{J=0} = 1; \tag{23}$$

$$F_{J=1} = \frac{\sqrt{1+R^2p_\mathrm{r}^2}}{\sqrt{1+R^2p_\mathrm{AB}^2}}; \tag{24}$$

$$F_{J=2} = \frac{\sqrt{9+3R^2p_\mathrm{r}^2+R^4p_\mathrm{r}^4}}{\sqrt{9+3R^2p_\mathrm{AB}^2+R^4p_\mathrm{AB}^4}}, \tag{25}$$

where $R$ is the radius of a meson. To be consistent with the previous Dalitz plot analyses at Belle [14], we have chosen $\mathrm{D}^0$ to have $R_\mathrm{D} = 5.0\ \mathrm{GeV}^{-1}$ and the intermediate resonances all to have $R_\mathrm{r} = 1.5\ \mathrm{GeV}^{-1}$. The momenta $p_\mathrm{r}$ and $p_\mathrm{AB}$ are for the decay form factor $F_\mathrm{r}$ given above. In the case of the birth form factor $F_\mathrm{D}$ the momenta $p_\mathrm{r}$ and $p_\mathrm{AB}$ are given by

$$\begin{aligned}p_\mathrm{AB} = &\frac{1}{2M_\mathrm{D}} \\ &\cdot\sqrt{[M_\mathrm{D}^2 - (m_\mathrm{AB}+M_\mathrm{C})^2][M_\mathrm{D}^2 - (m_\mathrm{AB}-M_\mathrm{C})^2]}\end{aligned} \tag{26}$$

$$p_\mathrm{r} = \frac{1}{2M_\mathrm{D}}\sqrt{[M_\mathrm{D}^2 - (M_\mathrm{r}+M_\mathrm{C})^2][M_\mathrm{D}^2 - (M_\mathrm{r}-M_\mathrm{C})^2]}, \tag{27}$$

where $M_\mathrm{r}$ is the nominal mass of the resonances, $m_\mathrm{AB}$ is the invariant mass of candidates, $M_\mathrm{C}$ is the nominal mass of $C$ final state particle and $M_\mathrm{D}$ is the nominal mass of the $\mathrm{D}^0$ meson. The parameters of the resonances are listed in Table 2 in this analysis.

### 3.2 Dalitz amplitude

The decay amplitude of $\mathrm{D}^0 \to \mathrm{K}\pi\pi^0$ as a function of Dalitz plot variables $m_{\mathrm{K}\pi}^2$ and $m_{\pi\pi^0}^2$ is expressed as a sum of quasi-two-body decay matrix elements and one non-resonant (NR) decay amplitude; $m_{\mathrm{K}\pi}^2 \equiv m_{\mathrm{K}^-\pi^+}^2$, $m_{\pi\pi^0}^2 \equiv m_{\pi^+\pi^0}^2$ in RS decay and $m_{\mathrm{K}\pi}^2 \equiv m_{\mathrm{K}^+\pi^-}^2$, $m_{\pi\pi^0}^2 \equiv m_{\pi^-\pi^0}^2$ in WS decay,

$$\mathcal{M}(m_{\mathrm{K}\pi}^2, m_{\pi\pi^0}^2) = \sum_\mathrm{r} a_\mathrm{r} \mathrm{e}^{\mathrm{i}\phi_\mathrm{r}} \mathcal{A}_\mathrm{r}(m_{\mathrm{K}\pi}^2, m_{\pi\pi^0}^2) + a_\mathrm{NR}\mathrm{e}^{\mathrm{i}\phi_\mathrm{NR}}, \tag{28}$$

Table 2. The parameters of all resonances used in our Dalitz plot fitting, including scalar, vector, tensor particles [1].

| resonances | $I^G(J^{PC})$ | mass/(GeV/$c^2$) | width/(GeV/$c^2$) | $R(F_\mathrm{r})/\mathrm{GeV}^{-1}$ | $R(F_\mathrm{D})/\mathrm{GeV}^{-1}$ |
|---|---|---|---|---|---|
| $\mathrm{K}_0^*(1430)^\pm$ | $1/2(0^+)$ | $1.425 \pm 0.050$ | $0.270 \pm 0.080$ | 1.5 | 5.0 |
| $\mathrm{K}_0^*(1430)^0$ | $1/2(0^+)$ | $1.425 \pm 0.050$ | $0.270 \pm 0.080$ | 1.5 | 5.0 |
| $\rho(770)^\pm$ | $1^+(1^{--})$ | $0.77549 \pm 0.00034$ | $0.1491 \pm 0.0008$ | 1.5 | 5.0 |
| $\rho(1450)^\pm$ | $1^+(1^{--})$ | $1.465 \pm 0.025$ | $0.400 \pm 0.060$ | 1.5 | 5.0 |
| $\rho(1700)^\pm$ | $1^+(1^{--})$ | $1.720 \pm 0.020$ | $0.250 \pm 0.100$ | 1.5 | 5.0 |
| $\mathrm{K}^*(892)^\pm$ | $1/2(1^-)$ | $0.89166 \pm 0.00026$ | $0.0508 \pm 0.0009$ | 1.5 | 5.0 |
| $\mathrm{K}^*(892)^0$ | $1/2(1^-)$ | $0.89594 \pm 0.00022$ | $0.0487 \pm 0.0008$ | 1.5 | 5.0 |
| $\mathrm{K}^*(1410)^\pm$ | $1/2(1^-)$ | $1.414 \pm 0.015$ | $0.232 \pm 0.021$ | 1.5 | 5.0 |
| $\mathrm{K}^*(1410)^0$ | $1/2(1^-)$ | $1.414 \pm 0.015$ | $0.232 \pm 0.021$ | 1.5 | 5.0 |
| $\mathrm{K}^*(1680)^\pm$ | $1/2(1^-)$ | $1.717 \pm 0.027$ | $0.332 \pm 0.110$ | 1.5 | 5.0 |
| $\mathrm{K}^*(1680)^0$ | $1/2(1^-)$ | $1.717 \pm 0.027$ | $0.332 \pm 0.110$ | 1.5 | 5.0 |
| $\mathrm{K}_2^*(1430)^\pm$ | $1/2(2^+)$ | $1.4256 \pm 0.0015$ | $0.0985 \pm 0.0027$ | 1.5 | 5.0 |
| $\mathrm{K}_2^*(1430)^0$ | $1/2(2^+)$ | $1.4324 \pm 0.0013$ | $0.109 \pm 0.005$ | 1.5 | 5.0 |

where each term is parameterized with an amplitude $a_{\rm r}$ and a phase $\phi_{\rm r}$. The function $\mathcal{A}_{\rm r}(m^2_{\rm K\pi},m^2_{\pi\pi^0})$ is the Lorentz-invariant expression for the matrix element.

The signal probability density function has the normalized form

$$p_{\rm sig}(m^2_{{\rm K}\pi,i},m^2_{\pi\pi^0,i}) = \frac{|\mathcal{M}(m^2_{{\rm K}\pi,i},m^2_{\pi\pi^0,i})|^2\cdot\epsilon(m^2_{\rm K\pi},m^2_{\pi\pi^0})}{\oint_D {\rm d}m^2_{\rm K\pi}{\rm d}m^2_{\pi\pi^0}|\mathcal{M}(m^2_{\rm K\pi},m^2_{\pi\pi^0})|^2\cdot\epsilon(m^2_{\rm K\pi},m^2_{\pi\pi^0})} \quad (29)$$

where the integral in the denominator is present for the overall normalization of the probability density, and $\epsilon(m^2_{\rm K\pi},m^2_{\pi\pi^0})$ is the efficiency to correct the Dalitz plot structure. The sensitivity estimation in this paper is performed at generator level, hence $\epsilon(m^2_{\rm K\pi},m^2_{\pi\pi^0})=1$.

### 3.3 Time-dependent Dalitz analysis

$\mathcal{M}^{\rm CF}_{\bar f}$ and $\mathcal{M}^{\rm DCS}_{\bar f}$ are used to describe the CF process decays and the DCS process decays in WS decay. According to the amplitude of WS decay $\rm D^0\to\bar f$ in Eq.(4),

$$\mathcal{M}(\bar f,t)=\langle\bar f|\mathcal{H}|{\rm D}^0(t)\rangle=\frac{1}{2}\left(\mathcal{M}^{\rm DCS}_{\bar f}+\frac{1}{r_0}\cdot{\rm e}^{{\rm i}\delta}\bar{\mathcal{M}}^{\rm CF}_{\bar f}\right)e_1(t) +\frac{1}{2}\left(\mathcal{M}^{\rm DCS}_{\bar f}-\frac{1}{r_0}\cdot{\rm e}^{{\rm i}\delta}\bar{\mathcal{M}}^{\rm CF}_{\bar f}\right)e_2(t). \quad (30)$$

To take into account the finite precision of lifetime at the Belle II detector, the time components of the time-dependent amplitude in Eq.(10) should be convoluted with time resolution function $Res(t)$. Hence, we have the time-dependent Dalitz plot fitting formalism in Eq.(31) with the time resolution:

$$\begin{aligned}|\mathcal{M}(\bar f,t)|^2=&|\mathcal{M}^{\rm DCS}_{\bar f}|^2\cdot{\rm e}^{-\Gamma t}\otimes_t Res(t)\\ &+\frac{x''^2+y''^2}{4}|\bar{\mathcal{M}}^{\rm CF}_{\bar f}|^2\frac{1}{r_0^2}\cdot(\Gamma^2t^2\cdot{\rm e}^{-\Gamma t})\otimes_t Res(t)\\ &-\frac{1}{r_0}\cdot(y''\cdot{\rm Re}[\mathcal{M}^{\rm DCS}_{\bar f}\bar{\mathcal{M}}^{*\,{\rm CF}}_{\bar f}]+x''\\ &\cdot{\rm Im}[\mathcal{M}^{\rm DCS}_{\bar f}\bar{\mathcal{M}}^{*\,{\rm CF}}_{\bar f}])(\Gamma t\cdot{\rm e}^{-\Gamma t})\otimes_t Res(t). \quad (31)\end{aligned}$$

Three functions of the time component are defined as

$$Ep_0(t;\tau)=\frac{1}{\tau}{\rm e}^{-t/\tau};\quad Ep_1(t;\tau)=\frac{t}{\tau^2}{\rm e}^{-t/\tau};\quad Ep_2(t;\tau)=\frac{t^2}{2\tau^3}{\rm e}^{-t/\tau} \quad (32)$$

and their normalisations in the time region $[a,b]$ are respectively

$$NEp_0=\int_a^b Ep_0(t,\tau){\rm d}t=\tau\Big(Ep_0(a)-Ep_0(b)\Big), \quad (33)$$

$$NEp_1=\int_a^b Ep_1(t,\tau){\rm d}t=\tau\Big(Ep_1(a)-Ep_1(b)\Big)+NEp_0, \quad (34)$$

$$NEp_2=\int_a^b Ep_2(t,\tau){\rm d}t=\tau\Big(Ep_2(a)-Ep_2(b)\Big)+NEp_1. \quad (35)$$

A Gaussian function is used as the time resolution. With two parameters defined, $X$ and $Z$,

$$X=\frac{1}{2}\left(\frac{\sigma}{\tau}\right)^2-\frac{t-\mu}{\tau},\qquad Z=\frac{1}{\sqrt{2}}\left(\frac{\sigma}{\tau}-\frac{t-\mu}{\sigma}\right) \quad (36)$$

the convolution of the $Ep_i$ (i=0, 1, 2) with time resolution respectively is

$$R_0(t)=Ep_0\otimes_t Res(t)=\frac{1}{2\tau}{\rm e}^X{\rm erfc}(Z) \quad (37)$$

$$R_1(t)=Ep_1\otimes_t Res(t)=\frac{\sqrt{2}\sigma}{2\tau^2}{\rm e}^X\left[\frac{1}{\sqrt{\pi}}{\rm e}^{-Z^2}-Z\,{\rm erfc}(Z)\right] \quad (38)$$

$$R_2(t)=Ep_2\otimes_t Res(t)=\frac{\sigma^2}{2\tau^3}{\rm e}^X\left[\left(Z^2+\frac{1}{2}\right){\rm erfc}(Z)-\frac{Z}{\sqrt{\pi}}{\rm e}^{-Z^2}\right] \quad (39)$$

and the $R_i(t)$ normalisations of time region $[a,b]$ respectively are

$$NR_0=\int_a^b\frac{1}{2\tau}{\rm e}^X{\rm erfc}(Z){\rm d}t=\tau\Big(R_0(a)-R_0(b)\Big)+\frac{1}{2}\left[{\rm erf}\left(\frac{(b-\mu)}{\sqrt{2}\sigma}\right)-{\rm erf}\left(\frac{a-\mu}{\sqrt{2}\sigma}\right)\right] \quad (40)$$

$$NR_1=\int_a^b\frac{\sqrt{2}\sigma}{2\tau^2}{\rm e}^X\left[\frac{1}{\sqrt{\pi}}{\rm e}^{-Z^2}-Z\,{\rm erfc}(Z)\right]{\rm d}t=\tau\Big(R_1(a)-R_1(b)\Big)+NR_0 \quad (41)$$

$$NR_2=\int_a^b\frac{\sigma^2}{2\tau^3}{\rm e}^X\left[\left(Z^2+\frac{1}{2}\right){\rm erfc}(Z)-\frac{Z}{\sqrt{\pi}}{\rm e}^{-Z^2}\right]{\rm d}t=\tau\Big(R_2(a)-R_2(b)\Big)+NR_1. \quad (42)$$

The $i^{\rm th}$ event's normalised probability density function of the time-dependent Dalitz plot is Eq.(43) with efficiency plane correction:

$$p_{\rm sig}(m^2_{{\rm K}\pi,i},m^2_{\pi\pi^0,i},t_i)=\frac{\left|\mathcal{M}(m^2_{{\rm K}\pi,i},m^2_{\pi\pi^0,i},t_i)\otimes_t Res(t_i)\right|^2\epsilon(m^2_{{\rm K}\pi,i},m^2_{\pi\pi^0,i})}{\int{\rm d}t\oint_D{\rm d}m^2_{\rm K\pi}{\rm d}m^2_{\pi\pi^0}\ \left|\mathcal{M}(m^2_{\rm K\pi},m^2_{\pi\pi^0},t)\otimes_t Res(t)\right|^2\epsilon(m^2_{\rm K\pi},m^2_{\pi\pi^0})}. \quad (43)$$

The Input/Output checks are usually given at generator level and reconstruction level. The time-dependent Dalitz plot fitting uses the unbinned maximum likelihood method:

$$-2\cdot\ln\mathcal{L}=-2\sum_{i=1}^{N}\ln\ p_{\rm sig}(m^2_{{\rm K}\pi,i},m^2_{\pi\pi^0,i},t_i;x,y). \quad (44)$$

## 4 The Belle II detector at SuperKEKB

SuperKEKB, a next-generation B factory (also a tau-charm factory), follows its predecessor KEKB, which collected about 1 ab$^{-1}$ of data and achieved a world record for instantaneous luminosity of $2.1\times10^{34}$ cm$^{-2}$s$^{-1}$. It aims to achieve an instantaneous peak luminosity of $8\times10^{35}$ cm$^{-2}\cdot$s$^{-1}$ and collect 50 ab$^{-1}$ of experimental data.

To improve the vertex resolution significantly, the Belle II detector [15] has a new vertex detector system including a two-layer pixel vertex detector (PXD), whose innermost layer nearer the IP is about 1.4 cm, and a four-layer double-sided silicon-strip detector (SVD), whose outermost SVD layer is located at a larger radius than at Belle, resulting in higher reconstruction efficiency for $K^0_S$ mesons. A new central drift chamber (CDC) has been built with smaller cell sizes than Belle's, which has significant improvement against the higher level of beam background. Combined with the vertex detectors, Belle II has better $D^*$ meson reconstruction efficiency. Belle II uses squeezed beams at the interaction point (IP) and the size of the beam-spot is two orders of magnitude smaller than at Belle and BaBar. This will improve the constraint for the decay chain vertex fitting.

According to MC studies [16], Belle II has a factor of two improvement in proper time resolution over Belle and BaBar ($\sigma_t=270$ fs). In this estimation analysis, a Gaussian with width $\sigma_t=140$ fs is used as the Belle II input on proper time resolution $Res(t)$.

## 5 Mixing sensitivity estimation for Belle II

To obtain signal MC samples, the EvtGen [17] package, which is an event generator designed to simulate the physics of B decays, is expanded with a time-independent Dalitz generator for the RS decay $D^0\to K^-\pi^+\pi^0$ and a time-dependent Dalitz generator for the WS decay $D^0\to K^+\pi^-\pi^0$.

Firstly, a RS signal MC sample is produced by the RS decay generator with an amplitude described by eleven resonances[1)] and a nonresonance Dalitz model, referring to the Dalitz fitting result on the $D^0\to K^-\pi^+\pi^0$ RS sample with the Belle dataset [18]. Then a time-independent Dalitz analysis is performed and the fitted RS parameters are consistent with the input values in the MC generator. The fitting fractions of each resonance are also checked and are consistent with the input values. On all Dalitz variables and lifetime projections, the fitting results can describe the distribution well. This RS amplitude will be used for the CF process $\mathcal{M}^{\rm CF}_{\bar f}$ with conjugated decays in the WS decay generator.

Secondly, a seven-resonance Dalitz model, referring to BaBar's measurement [9], is used to parameterise the DCS process $\mathcal{M}^{\rm DCS}_{f}$. The mixing parameters $(x,\ y,\ \delta,\ 1/r_0)=(0.0258,\ 0.0039,\ 10^\circ,\ 13.8)$ in Eq. (30) are fixed as the WS generator input parameters. Assuming similar efficiency to BaBar, it is estimated that Belle II will collect at least 225000 signal events with the full 50 ab$^{-1}$ dataset. To get a reliable sensitivity estimation, the MC sample is kept the same as this estimated number. A time-dependent Dalitz analysis (TDDA) on this WS sample was performed successfully. The fitted WS parameters, especially the mixing parameters with which we are concerned, show no significant bias within the uncertainty by comparing the input values.

The time resolution has non-negligible effects on the time-dependent amplitude analyses. Thirdly, the $D^0$ lifetime $t$ is smeared by the resolution function $Res(t)=$ Gauss with a width $\sigma=140$ fs. Then TDDA on the signal MC sample based on Eq.(44) is performed. The Dalitz plot and lifetime projections of time-dependent Dalitz fitting are shown in Fig. 3.

Finally, the TDDA is duplicated on ten sets of time-smeared signal Dalitz MC samples. The two mixing parameters are extracted and shown in Fig. 4 (left). The projections of x and y separately are given in Fig. 4. The RMS value of these projections are obtained as the mixing parameters' expected uncertainty: $\sigma_x=0.057\%$, and $\sigma_y=0.049\%$ for a 50 ab$^{-1}$ dataset. According to TDDA of WS decays at Belle, the backgrounds will affect this statistical uncertainty. As we lack these background samples, we conclude that the integrated luminosity of 50 ab$^{-1}$ dataset at Belle II can improve the statistical uncertainty by at least one magnitude for the mixing parameters, without considering the background effects. According to our studies at Belle, we estimate that the fitted statistical uncertainty will be affected by the backgrounds and result in an increase of about $<40\%$.

1) In this WS decay, there are thirteen possible resonances shown in Table 2, but referring to the Dalitz analysis of RS decay at Belle [18], ρ(1450) and ρ(1700) have masses whose peaks are both outside the Dalitz plot but whose widths are so wide that their tails extend well into the region of interest. Since their fitted phase angles difference is very close to 180°, the fitting will be unable to separate them. We keep only ρ(1700) instead of both, which is same choice as CLEO [12]. We also remove $K^*(1680)^0$, because of its very small contribution to the total amplitude, with a fitting fraction less than 0.1% [18].

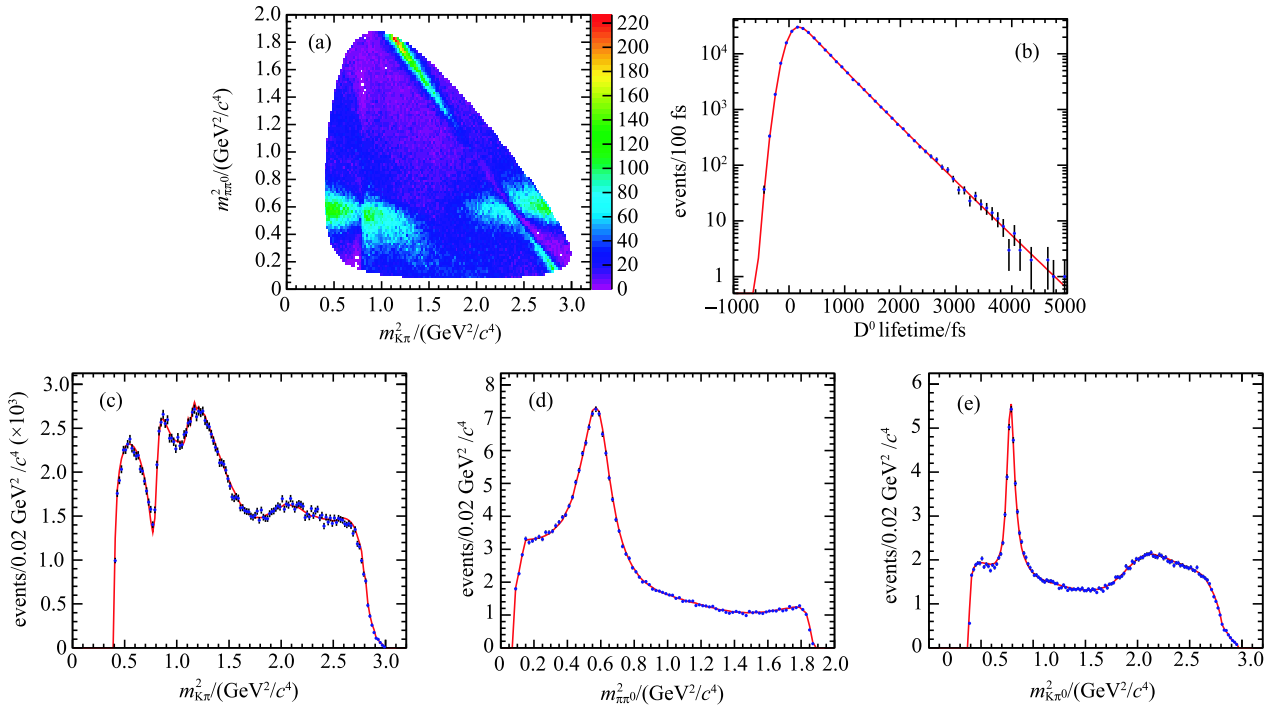


Fig. 3. (color online)The time-dependent Dalitz fitting on a Dalitz signal MC sample with time smeared: (a) 2-dimensional Dalitz plot; (b) lifetime projection; and projections of Dalitz variables $m^2_{\mathrm{K}\pi}$(c), $m^2_{\pi\pi^0}$(d) and $m^2_{\mathrm{K}\pi^0}$(e).

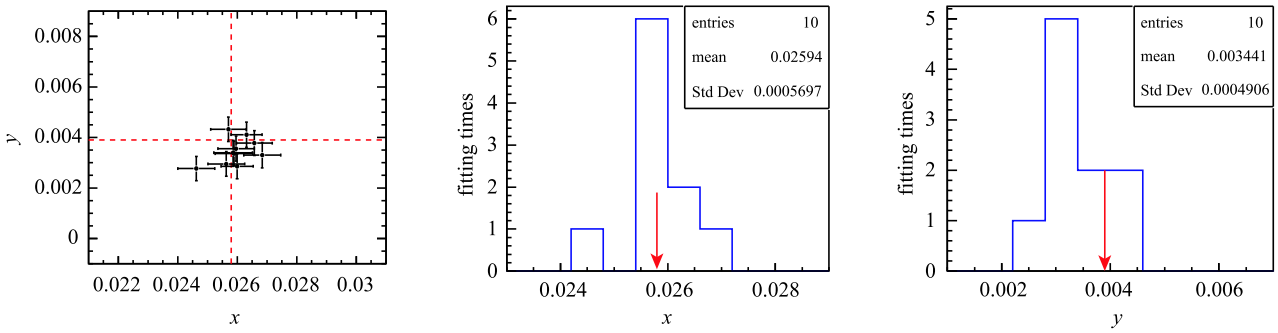


Fig. 4. The time-dependent Dalitz plot fitting results (the intersection of the dashed lines is the input value in the generator) for mixing parameters of ten sets of Dalitz signal MC (each set with 225000 events) with time smeared. The projections of $x$ and $y$ are shown with the standard deviation value (Std Dev) as our estimation of $x$ and $y$ errors (the arrows are input values).

Here we estimate the effect on systematic uncertainty by statistical data. Referring to BaBar's measurement [9], $x'/r_0 = 0.353 \pm 0.091 \pm 0.066$ and $y'/r_0 = -0.002 \pm 0.090 \pm 0.057$ with determination $r_0^2 = (5.25^{+0.25}_{-0.31} \pm 0.12) \times 10^{-3}$. The main sources of systematic uncertainties are listed below for experimental detection systematic uncertainties and systematic uncertainties related to the parameterization of Dalitz distribution of $\mathrm{D}^0 \to \mathrm{K}^+\pi^-\pi^0$ decays [19]:

1) Reducible systematic uncertainties:

– The uncertainties from the parameterization of WS CF amplitude, which uses the result from RS Dalitz fit, are estimated by varying the parameters of $\pm\sigma$: $\sigma_{x'/r_0} = 0.23\sigma$ and $\sigma_{y'/r_0} = 0.22\sigma$.

– The "signal and background number" uncertainty: $\sigma_{x'/r_0} = 0.15\sigma$ and $\sigma_{y'/r_0} = 0.22\sigma$ [1)].

– The "resolution function" systematics is estimated by using different resolution function parameterizations: $\sigma_{x'/r_0} = 0.11\sigma$ and $\sigma_{y'/r_0} = 0.09\sigma$. A larger data sample will enable better determination of the resolution

1) here $\sigma$ is the statistical uncertainty of parameters $x'/r_0$ or $y'/r_0$ correspondingly.

function quality.

- The "combinatorial background" parameterization uncertainty from the sideband region: $\sigma_{x'/r_0} = 0.02\sigma$ and $\sigma_{y'/r_0} = 0.00\sigma$.
- Variations in efficiency across the Dalitz plot contribute to systematic uncertainties of $\sigma_{x'/r_0} = 0.09\sigma$ and $\sigma_{y'/r_0} = 0.10\sigma$.

2) Irreducible systematic uncertainties:

- The largest error arises from the choices of "lifetime $t$ region" and "lifetime error $\sigma_t$ region": $\sigma_{x'/r_0} = 0.48\sigma$ and $\sigma_{y'/r_0} = 0.31\sigma$. [1)].
- The definition of the signal region has non-negligible effects on systematic uncertainties: $\sigma_{x'/r_0} = 0.15\sigma$ and $\sigma_{y'/r_0} = 0.19\sigma$.
- Dalitz model by using alternative parameterizations, especially using a Breit-Wigner function and a flat non-resonant contribution instead of LASS paramterization of the Kπ $S$-wave, contributes the systematic uncertainties: $\sigma_{x'/r_0} = 0.22\sigma$ and $\sigma_{y'/r_0} = 0.24\sigma$.

The systematics uncertainty can be roughly estimated by formalism as

$$\sigma_{\rm syst} = \sqrt{\sigma^2_{\rm red.} \times 384\ fb^{-1}/50\ ab^{-1} + \sigma^2_{\rm irred.}}. \qquad (45)$$

Because Belle II will have almost 130 times as large a dataset as for the BaBar measurement, these reducible systematic uncertainties can be reduced by about an order of magnitude. Therefore the systematic uncertainty can be reduced about 20% for $x'/r_0$ and $y'/r_0$ as our conservative estimation.

## 6 Summary

In conclusion, by considering the time resolution improvement ($\sigma_t = 140$ fs) of the Belle II detector at SuperKEKB and using time-dependent Dalitz plot fitting, $\rm D^0$-$\bar{\rm D}^0$ mixing sensitivity estimation for the WS decay $\rm D^0 \to K^+\pi^-\pi^0$ using the Belle II 50 $\rm ab^{-1}$ dataset is presented with $\sigma_x = 0.057\%$ and $\sigma_y = 0.049\%$ under the condition of $\delta = 10^\circ$ and $1/r_0 = 13.8$ fixed. This will give an order of magnitude improvement for mixing parameters without considering the background effects. A larger statistical dataset will reduce systematic uncertainties at least 20% for $x'/r_0$ and $y'/r_0$ compared to BaBar's measurement.

*We thank the Belle collaboration for supplying the EvtGen package. Our Dalitz generator is based on and expands this package. We also thank the Belle II collaboration, especially Prof. Alan Schwartz and Prof. Giulia Casarosa, for the study of* $\rm D^0$ *lifetime resolution in the Belle II detector.*

## References

1 K. A. Olive et al (Particle Data Group), Chin. Phys. C, **38**: 090001 (2014)
2 Xing Zhi-Zhong, Chin. Phys. C, **32**: 483-487 (2008)
3 S. L. Glashow, J. Iliopoulos, and L. Maiani, Phys. Rev. D, **2**: 1285 (1970)
4 A. F. Falk et al, Phys. Rev. D, **65**: 054034 (2002)
5 R. Aaij et al (LHCb Collaboration), Phys. Rev. Lett., **111**: 241801 (2013)
6 T. Aaltonen et al (CDF Collaboration), Phys. Rev. Lett., **111**: 231802 (2013)
7 B. R. Ko et al (Belle Collaboration), Phys. Rev. Lett., **112**: 111801 (2014)
8 R. Aaij et al (LHCb Collaboration), Phys. Rev. Lett., **116**: 241801 (2016)
9 B. Aubert et al (BaBar Collaboration), Phys. Rev. Lett., **103**: 211801 (2009)
10 Boštjan Golob, Karim Trabelsi, and Philip Urquijo, BELLE2-NOTE-0021
11 X. C. Tian et al (Belle Collaboration), Phys. Rev. Lett., **95**: 231801 (2005)
12 S. Kopp et al (CLEO Collaboration), Phys. Rev. D, **63**: 092001 (2001)
13 Charles Zemach, Phys. Rev., **133**: B1201 (1964); Charles Zemach, Phys. Rev., **140**: B109 (1965)
14 T. Peng et al (Belle Collaboration), Phys. Rev. D, **89**: 091103(R) (2014)
15 T. Abe et al KEK Report 2010-1, arXiv:1011.0352 [physics.ins-det]
16 G. Casarosa, Belle II Decay Time Resolution, Presented at the 2nd Belle II Theory Interface Platform Workshop (Krakow, April 2015)
17 D. J. Lange, Nucl. Instrum. Methods A, **462**: 152-155 (2001)
18 L. K. Li, W. B. Yan, and Z. P. Zhang, Belle Note 1381
19 M. Pelliccioni, *Measurement of* $\rm D^0$-$\bar{\rm D}^0$ *Mixing with a Time-Dependent Amplitude Analysis of* $\rm D^0 \to K^+\pi^-\pi^0$, SLAC-R-1017, Ph. D. Thesis (SLAC National Accelerator Laboratory, Stanford University, Stanford CA 94309, 2009)

1) These systematic uncertainties should be decreased as Belle II has a better time resolution.